Table 4 indicates the effect of the beam diameter (1.25, 2.5 and 5 mm) with a fixed energy spread of 5%. The maximum and minimum values of the depth spacing were almost constant, as anticipated from the fixed energy spread. Also, the beam diameter affected the lateral spacing, as expected. The number of beams and target spots decreased significantly with an increase in the beam diameter. For a beam of 1.25 mm, nearly a thousand target spots were generated by the planning software. Such a large number of target spots would likely require a lot of time to treat.

A histogram of particle energy for a typical treatment plan is displayed in Fig. 7. In general, more particles at the higher-energy end of the spectrum are necessary because more particles are targeted at deeper locations in forming the SOBP. The energy distribution is also affected by the target shape and the incident beam direction. The energy distribution is not smooth, partly due to the discrete proton energy values used for our calculations.

**Table 1** Dosimetric characteristics: energy spread

| Energy spread | 5% | 10% | 15% |
|---|---|---|---|
| Retina ≥45 CGE | 1% | 2% | 5% |
| Lens ≥10 CGE | 0% | 0% | 0% |
| Optic nerve ≥12 CGE | 10% | 20% | 31% |
| Dose at macula (≥30 CGE) | 27 (OK) | 36 (NG) | 42 (NG) |
| Dose at optic disc (≥12 CGE) | 11 (OK) | 1.8 (OK) | 3.3 (OK) |
| V95[a] | 98% | 98% | 97% |

[a] Percentage volume of PTV, which received 95% of the prescribed dose (57 CGE)

**Table 2** Target spot and beam characteristics: energy spread

| Energy spread | 5% | 10% | 15% |
|---|---|---|---|
| Lateral spacing (mm) | 1.3 | 1.3 | 1.3 |
| Depth spacing, minimum (mm) | 0.6 | 1.7 | 3.1 |
| Depth spacing, maximum (mm) | 2.8 | 5.8 | 9.1 |
| Number of beams | 38 | 38 | 38 |
| Number of target spots | 239 | 102 | 65 |

Beamlet diameter was 2.5 mm for each case

## 4 Discussion

Many parameters and parameter combinations (such as beam diameter, energy spread, lateral spacing, depth spacing, number of beams and number of target spots) must be considered in assessing proton treatment of small superficial tumors. Realistically, some of the parameters may need to be predetermined in the clinical equipment because of mechanical or other limitations. In this study, we simulated the effect of energy spread by using a fixed beam diameter (2.5 mm), and the effect of the beam diameter by using a fixed energy spread (5%). These values were chosen because they seemed to be the most likely parameters delivered by an actual accelerator. A more thorough parameter survey is necessary for determination of the effects of every possible combination of beam parameters.

For reducing treatment times, it is desirable to reduce the number of target spots in a plan. However, there is a trade-off between the dose distribution and the number of target spots. Our results suggest that, if the beam energy and lateral spacing are predetermined, the energy spread and beam diameters must be chosen carefully with this in mind. The clinical significance of dose–volume statistics of the PTV and organs at risk must be determined for each patient.

The dose distributions shown here contain many hot spots (overdose areas). These are caused partially by the histogram normalization method, where 95% of the target volume is forced to receive at least 100% of the prescribed dose. Without normalization, cold spots were prevalent around the lateral and distal edges, especially when a large beam diameter or energy spread was used. The cold spots became prevalent when the distance from the tumor polygon edge and nearest target spot was relatively large. This resulted in DVH curves for the target volume not being as steep (selective) as they should have been. Several methods can be employed for improving the dose distributions,

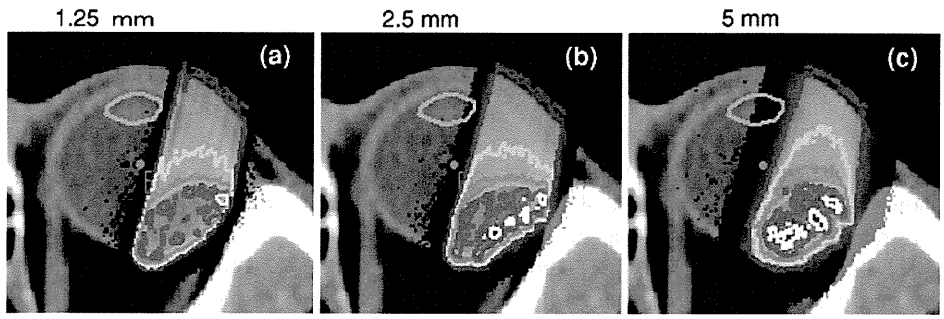


**Fig. 5** Dose distribution for various values for beam diameter, 1.25 mm (**a**) 2.5 mm (**b**), and 5 mm (**c**). Isodose lines are 125% of prescribed dose (75 CGE) *white*, 110% (66 CGE) *red*, 90% (54 CGE) *orange*, 75% (45 CGE) *yellow* and 50% (30 CGE) *blue*. In all cases, we used 5% energy spread (color figure online)

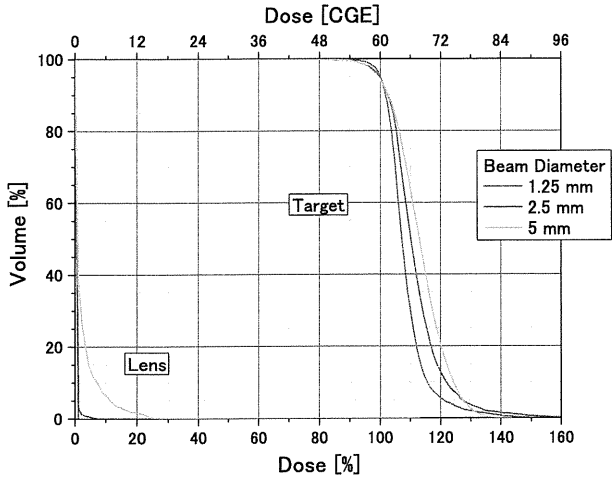


**Fig. 6** DVH for PTV and optic nerve computed with various values for beam diameter. In all cases, we used 5% energy spread (color figure online)

**Table 3** Dosimetric characteristics: beam diameter

| Beam diameter | 1.25 mm | 2.5 mm | 5 mm |
|---|---|---|---|
| Retina ≥45 CGE | 0% | 0% | 1% |
| Lens ≥10 CGE | 0% | 0% | 6% |
| Optic nerve ≥12 CGE | 0% | 1% | 4% |
| Dose at macula (≥30 CGE) | 13 (OK) | 13 (OK) | 36 (NG) |
| Dose at optic disc (≥12 CGE) | 0.8 (OK) | 3.0 (OK) | 18 (NG) |
| V95[a] | 99% | 98% | 98% |

[a] Percentage volume of CTV, which received 95% of the prescribed dose (57 CGE)

**Table 4** Spot and beam characteristics: beam diameter

| Beam diameter | 1.25 mm | 2.5 mm | 5 mm |
|---|---|---|---|
| Lateral spacing (mm) | 0.7 | 1.4 | 2.6 |
| Depth spacing, minimum (mm) | 0.7 | 0.7 | 0.6 |
| Depth spacing, maximum (mm) | 2.4 | 2.4 | 2.3 |
| Number of beams | 206 | 57 | 21 |
| Number of target spots | 918 | 233 | 87 |

Energy spread was 5% for each case

including increasing the number of Monte Carlo events, decreasing the space between target spots and improving the optimization algorithm. Furthermore, we used a fixed spacing factor of 0.5 in this study. Introduction of a variable spacing factor for each beam may further improve the homogeneity of dose distributions. The spacing factor should be smaller near the polygon edges to prevent cold spots while maintaining a reasonable total number of spots. These are topics for future study.

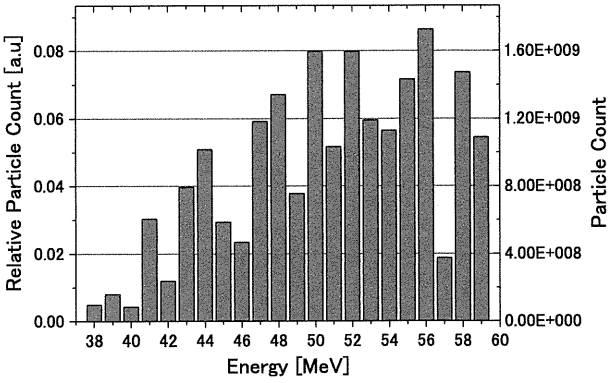


**Fig. 7** A typical histogram of particle energy levels (color figure online)

In this work, doses to the macula and to the optic disc were high and above the clinical limits in some cases. This is mainly because these structures are located directly behind the distal edge of the target volume. Proton spectra that are closer to being monoenergetic may improve the final clinical outcome. The effect of energy spread for deep-seated tumors such as prostate cancer may be different from that for shallow ocular diseases and is yet to be determined.

The required proton flux can be estimated as follows. Consider a shallow tumor volume of 1 cc (1 g). If the protons deposit an average energy of 50 MeV, then each proton delivers about $8 \times 10^{-12}$ J or $8 \times 10^{-9}$ Gy on average. Assuming an RBE of 1.1, each proton delivers about $9 \times 10^{-9}$ CGE. A typical treatment course consists of 60 CGE delivered in four fractions on consecutive days. If the irradiation time is limited to 1 min, then the accelerator must deliver 15 CGE per min or .25 CGE per s. The accelerator must therefore produce about 30 million protons per second or 4.8 pA. If such a delivery was carried out in 100 Hz repetitive pulsed laser shots, the required delivery would be in the order of $3 \times 10^5$ protons per shot.

## 5 Conclusion

Our simulations show that a 2.5-mm beam diameter and a 5% energy spread can be considered as a starting point for ocular cases. The dose distributions suggest that there is merit in continuing such parameter studies and considering further the potential for spot scanning proton sources.

**Acknowledgments** This work was supported by the Core Research for Evolutional Science and Technology (CREST), the Japan Science and Technology Agency (JST) and the Special Coordination Fund (SCF) for Promoting Science and Technology commissioned by the Ministry of Education, Culture, Sports, Science and Technology (MEXT) of Japan. K. S. is a Takuma Scholar of PMRC.

## References


1. Brenner DJ, Hall EJ. Secondary neutrons in clinical proton radiotherapy: a charged issue. Radiat Oncol. 2008;86(2):165–70.
2. Kanai T, Kawachi K, Kumamoto Y, Ogawa H, Yamada Y, Matsuzawa H. Spot scanning system for proton radiotherapy. Med Phys. 1980;7(4):365–9.
3. Lomax AJ, Bohringer T, Bolsi A, Coray D, Emert F, Goitein G, et al. Treatment planning and verification of proton therapy using spot scanning: initial experiences. Med Phys. 2004;31(11):3150–7.
4. Lomax AJ, Boehringer T, Coray A, Egger E, Goitein G, Grossmann M, et al. Intensity-modulated proton therapy: a clinical example. Med Phys. 2000;28(3):317–24.
5. Tajima T. Prospect for compact medical laser accelerators. J Jpn Soc Therap Radiat Oncol. 1997;9(Suppl 2):83–5.
6. Malka V, Sven F, Lefebvre E, d'Humieres E, Ferrand R. Practicability of proton therapy using compact laser systems. Med Phys. 2004;31(6):1587–92.
7. Ma CM, Maughan RL. Point/counterpoint: within the next decade conventional cyclotrons for proton radiotherapy will become obsolete and replaced by far less expensive machines using compact laser systems for the acceleration of the protons. Med Phys. 2006;33(3):571–3.
8. Bulanov SV, Esirkepov T, Khoroshkov VS, Kuznetsov AV, Pegoraro F. Oncological hadrontherapy with laser ion accelerators. Phys Lett A. 2002;299:240–7.
9. Agostinelli S, Allisonas J, Amakoe K, Apostolakisa J, Araujo H, et al. Geant4–a simulation toolkit. Nucl Instrum Methods Phys Res A. 2003;506:250–303.
10. Carrier J, Archambault L, Beaulieu L, Roy R. Validation of Geant4, an object-oriented Monte Carlo toolkit, for simulations in medical physics. Med Phys. 2004;31(3):484–92.
11. Jiang H, Paganetti H. Adaptation of Geant4 to Monte Carlo dose calculations based on CT data. Med Phys. 2004;31(10):2811–8.
12. Sutherland K, Miyajima S, Date H. A simple parallelization of Geant4 on a PC cluster with static scheduling for dose calculations. First European workshop on Monte Carlo treatment planning, Journal of Physics: Conference Series. 2007; 74 012020.
13. Schneider W, Bortfeld T, Schlegel W. Correlation between CT numbers and tissue parameters needed for Monte Carlo simulations of clinical dose distributions. Phys Med Biol. 2000;45:459–78.
14. Iwase H, Niita K, Nakamura T. Development of a general-purpose particle and heavy ion transport Monte Carlo code. J Nucl Sci Technol. 2002;39(11):1142–51.
15. Niita K, Sato T, Iwase H, Nose H, Nakashima H, Sihver L. PHITS: a particle and heavy ion transport code system. Radiat Meas. 2006;41:1080–90.
16. Dendale R, et al. Proton beam radiotherapy for uveal melanoma: results of Curie Institute-Orsay Proton Therapy Center (ICPO). Int J Radiat Oncol Biol Phys. 2006;65(3):780–7.

Int. J. Radiation Oncology Biol. Phys., Vol. 77, No. 2, pp. 630–636, 2010

0360-3016/$–see front matter

ELSEVIER

doi:10.1016/j.ijrobp.2009.08.060

**PHYSICS CONTRIBUTION**

# EVALUATION OF THE EFFECTIVENESS OF THE STEREOTACTIC BODY FRAME IN REDUCING RESPIRATORY INTRAFRACTIONAL ORGAN MOTION USING THE REAL-TIME TUMOR-TRACKING RADIOTHERAPY SYSTEM

GERARD BENGUA, PH.D.,* MASAYORI ISHIKAWA, PH.D.,* KENNETH SUTHERLAND,* KENJI HORITA, R.T.,† RIE YAMAZAKI, R.T.,† KATSUHISA FUJITA, R.T.,† RIKIYA ONIMARU, M.D.,‡ NORIWO KATOH, M.D.,‡ TETSUYA INOUE, M.D.,‡ SHUNSUKE ONODERA, M.D.,‡ AND HIROKI SHIRATO, M.D.‡

From the *Department of Medical Physics, †Radiology Department, and ‡Graduate School of Medicine, Hokkaido University, Sapporo, Hokkaido, Japan

**Purpose: To evaluate the effectiveness of the stereotactic body frame (SBF), with or without a diaphragm press or a breathing cycle monitoring device (Abches), in controlling the range of lung tumor motion, by tracking the real-time position of fiducial markers.**

**Methods and Materials: The trajectories of gold markers in the lung were tracked with the real-time tumor-tracking radiotherapy system. The SBF was used for patient immobilization and the diaphragm press and Abches were used to actively control breathing and for self-controlled respiration, respectively. Tracking was performed in five setups, with and without immobilization and respiration control. The results were evaluated using the effective range, which was defined as the range that includes 95% of all the recorded marker positions in each setup.**

**Results: The SBF, with or without a diaphragm press or Abches, did not yield effective ranges of marker motion which were significantly different from setups that did not use these materials. The differences in the effective marker ranges in the upper lobes for all the patient setups were less than 1mm. Larger effective ranges were obtained for the markers in the middle or lower lobes.**

**Conclusion: The effectiveness of controlling respiratory-induced organ motion by using the SBF+diaphragm press or SBF + Abches patient setups were highly dependent on the individual patient reaction to the use of these materials and the location of the markers. They may be considered for lung tumors in the lower lobes, but are not necessary for tumors in the upper lobes. © 2010 Elsevier Inc.**

**Organ motion, Body frame, Real-time tracking, Effective range.**

## INTRODUCTION

The risk of radiation-induced lung complications may be minimized if intrafractional tumor motion caused by respiration during irradiation can be accurately accounted for. Various approaches to the management of respiratory motion in radiation therapy are comprehensively discussed in the American Association of Physicists in Medicine (AAPM) Report 91 (1). These include the accurate tracking of organ and tumor motion during treatment and methods by which the motion may be restricted or dampened.

Motion tracking may be accomplished by taking two sets of fluoroscopic images of the tumor itself, other anatomical structures, or fiducial markers placed near the tumor (2–4). Ideally, the function of real-time tracking is to determine the full range of tumor motion, as well as its trajectory during treatment from these fluoroscopic images taken at high frequency. At present, this is only possible in a few centers that have facilities dedicated for this purpose, such as the real-time tumor-tracking radiation therapy system developed at Hokkaido University Hospital (5, 6).

Restriction of respiration, on the other hand, can be achieved by using patient immobilization and by applying abdominal pressure. In extracranial stereotactic irradiation, Lax *et al.* (7), Herfarth *et al.* (8), and Negoro *et al.* (9) have reported the effectiveness of an abdominal press in reducing respiratory-induced tumor movement in stereotactic conformal radiation therapy of body tumors. Alternatively, an

Reprint requests to: Gerard Bengua, Department of Medical Physics, Hokkaido University Hospital, North-15 West-7, Kita-ku, Sapporo, 060-8648, Japan. Tel: (+81) 11-706-7638; Fax: (+81) 11-706-7639; E-mail: gerard@med.hokudai.ac.jp

The physics part of this study was supported by the grant-in-aid from the Japanese Ministry of Education, Culture, Sports, Science and Technology; the clinical portion was supported by the grant-in-aid from the Japanese Ministry of Health and Welfare.

Conflict of interest: This study was conducted in cooperation with Elekta Oncology Systems, Japan.

*Acknowledgment*—The authors express their gratitude to Drs. Shinichi Shimizu, Hiroshi Taguchi, and Mylin Torres for their help with the clinical aspects of this study.

Received Feb 18, 2009, and in revised form Aug 3, 2009. Accepted for publication Aug 19, 2009.

air-injected blanket has also been suggested for abdomen compression and fixation (10) to reduce breathing-induced organ motion.

In this study, we evaluated the effectiveness of a body frame and its combination with a diaphragm press in restricting the range of lung tumor motion by tracking the three-dimensional real-time position of fiducial gold markers embedded near the tumor. We also investigated the effect on respiratory-induced organ motion of using the stereotactic body frame (SBF) together with a breathing cycle monitoring device (Abches), which was used to self-regulate the patient's breathing cycle.

## MATERIALS AND METHODS

### *The real-time tumor-tracking radiotherapy system*

The three-dimensional trajectories of fiducial markers near or at tumor sites were tracked via the real-time tumor-tracking radiotherapy (RTRT) system at the Radiotherapy Department of Hokkaido University Hospital (5, 6, 11, 12). This fluoroscopy-based system is composed of two pairs of an X-ray source and image intensifier and an image acquisition and recognition unit that is interfaced with a linear accelerator to perform gated-irradiation. The positions of the gold markers were acquired every 0.033 s.

### *Body frame, diaphragm press, and breathing cycle monitor*

For patient immobilization, we used Elekta's SBF (Elekta Oncology Systems) (13, 14). The same body frame was used in an earlier investigation on respiratory tumor movement and setup error verification using X-ray simulator images (7, 9, 15). The SBF is made from a rigid material formed into a half-hexagonal shell that wraps around the patient's torso. Because of the restricted space inside the shell, the patient's arms had to be positioned outside the shell by raising them above the head. Patient fixation inside the body frame was accomplished by means of a vacuum pillow, the size of which was chosen to ensure that it could provide an exact fit to the patient's body contour.

An additional accessory to the SBF was a frame that supports a pentagonal plastic plate that can be placed against the patient's abdomen to restrict the diaphragm motion. The pressure applied by the plate was regulated depending on the tolerance of each patient and was used only in the part of our measurements where its effectiveness to control motion from respiration was evaluated.

A breathing cycle monitor (commercially available as Abches [APEX Medical Inc., Tokyo, Japan]) was also used in combination with the body frame to investigate whether self-regulated breathing can reduce the amplitude of respiratory-induced tumor and organ motion. As shown in Fig. 1, the Abches consists of two extended arms, one for detecting abdominal movement and the other for detecting chest movement, and a respiration range indicator visible to the patient through a mirror attached to the head during the measurement.

### *Patient demographics*

The patient population for this study was composed of 16 males and 3 females who were scheduled to undergo radiation therapy using the RTRT system in our hospital between 2006 and 2008. Table 1 shows the characteristics of the cohort for this study. The patients' ages ranged between 59 and 85 years (mean, 76 years). Fourteen patients had T1 lung cancer, whereas 5 had T2 and 1 had T3. No patient had lymph nodes irradiation and none of the patients had metastasis. Four patients had partial lung resection before the irradiation.

Table 1. Characteristics of the cohort for this study

| Parameters | Number of patients |
|---|---|
| Sex | |
| Male | 16 |
| Female | 3 |
| Age range | 59–85 (mean, 76) |
| Gold marker locations | |
| Upper right lobe | 5 |
| Middle lobe | 1 |
| Lower right lobe | 4 |
| Upper left lobe | 6 |
| Lower left lobe | 3 |
| Cancer classification | |
| T1N0M0 | 13 |
| T2N0M0 | 5 |
| T3N0M0 | 1 |

The locations of the gold markers were judged based on where they appeared in the computed tomography images of the patient. We classified the sample population into "upper lobe" or "middle or lower lobe" patients according to the location of gold markers in the lungs, because it has been reported that the relative locations in

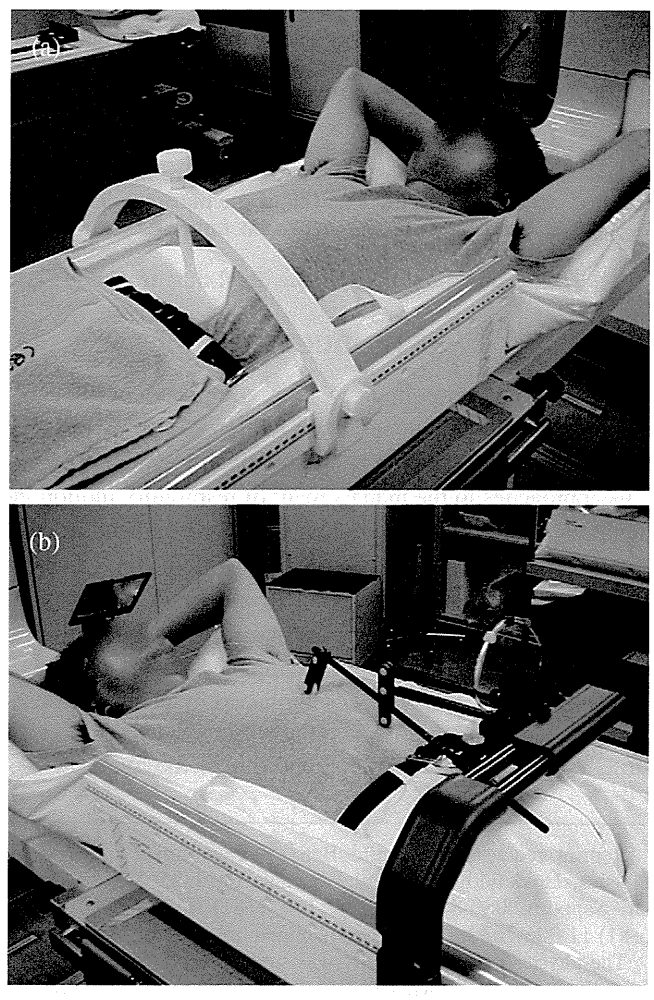


Fig. 1. Patient set-ups using the (a) stereotactic body frame (SBF)+diaphragm press (left) and the (b) SBF + Abches (right).

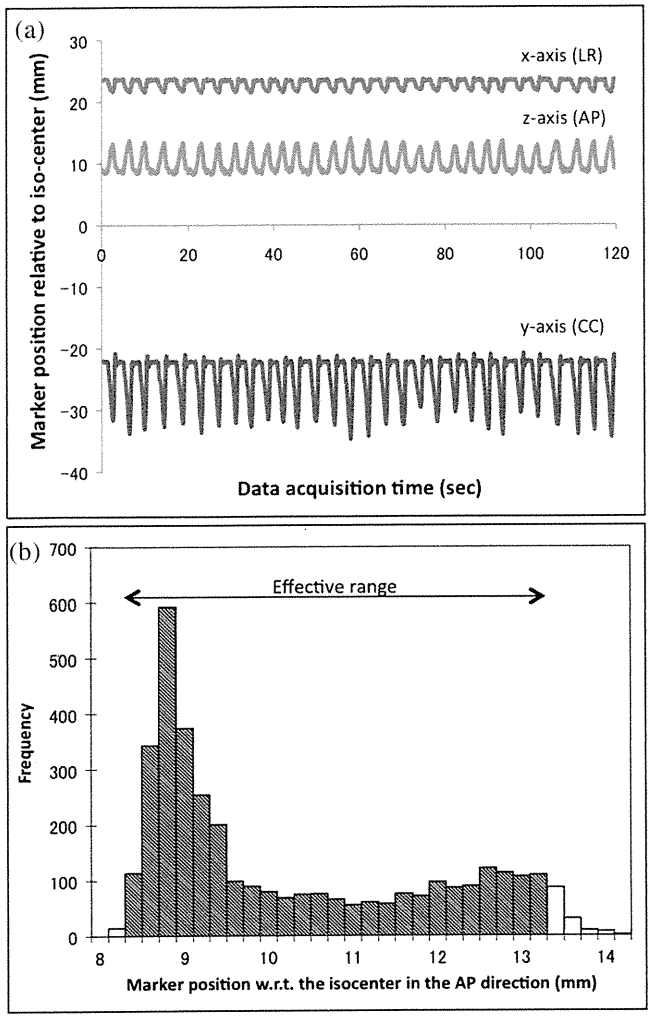


Fig. 2. Shown in (a) is an example of a 2-min tracking of the data from which the effective range was computed. The effective range along the z axis of the data in (a) is shown in (b).

the lung of the gold marker (16) and the tumor itself (17) influence the amplitude of their respective motions. Eleven of the 19 patients who participated in this study had gold markers embedded in the upper lobes of their lungs: 6 of the 11 had markers in the upper left and the other 5 had markers in the upper right. There was 1 patient with markers in the middle lobe and 7 patients with markers in either the lower left or lower right lobes of the lung.

*Patient setup*

Fluoroscopic tracking of the fiducial markers was performed in five different setups for each patient. In the first setup, the patient was made to lie on the treatment couch in the supine position with arms on the side. This was set as the reference patient position. In the second setup, the patient's arms were placed overhead to mimic the patient position when an SBF is used. The arms were not fixed into any structures, but were supported by cushions for patient comfort. The patient was asked to lie in the SBF in the third setup. Figure 1a shows the fourth setup, in which respiration was restricted using a plastic plate that pressed against the patient's diaphragm. In the fifth setup, shown in Fig. 1b, the Abches was attached to the SBF in the same manner as the abdominal press. The patients were able to monitor the relative amplitude of their breathing cycle from a respiration range indicator which was visible to the patient through a mirror.

*Marker tracking*

Tumor motion was monitored in real time by using 2-mm diameter gold markers, which were surgically placed near the tumor site and served as surrogate indicators of lung tumor motion (4). Three tracking measurements lasting for 5 min (2 min of tracking plus 3 min of rest) each were performed for every patient setup. The range of patient dose for the entire duration of marker tracking was between 14 and 591 mGy based on the estimates of Shirato *et al.* (18). Because the absorbed dose in the patient is strongly dependent on the tube voltage and pulse width, the X-ray tube settings were kept as low as possible during all the measurements.

*Evaluation index and statistical analysis*

The three-dimensional position of the gold marker relative to the iso-center is estimated by the RTRT system as it tracks the marker's motion. Sample tracking data are shown in Fig. 2a. The *effective range* of marker motion along each coordinate axis was computed about the mean marker position from the respective 2-min set of tracking data. Histograms similar to Fig. 2b with 0.2-mm position bins were constructed for each coordinate axis. The frequencies of the adjacent bins to the left and to the right of the median were accumulated until 95% of the total marker position frequency was achieved. The range of the included position bins was then defined as the *effective range* of the marker motion. The effective range along the z axis of the data in Fig. 2a is given as an example in Fig. 2b. A smaller effective range of the gold marker indicates less respiratory-induced organ motion.

The Mann-Whitney test was applied to assess the statistical significance of the differences in the effective ranges obtained between the reference setup and the other four setups.

This study was thoroughly discussed with the institutional review board of our hospital and its approval was received before the commencement of the measurements. Written patient consent was also received from all the participants in this research.

## RESULTS

The effective ranges were observed to vary from patient to patient. In the reference setup (no SBF-arms down setup), the range was 0.60–5.27 mm, 0.93–19.93 mm, and 1.00–10.20 mm along the left-right (LR), craniocaudal (CC), and anteroposterior (AP) directions, respectively, among the 19 patients. The tumor motion, as indicated by the effective range of the tracked gold marker, was reduced in some patients by changing the patient setup, such as by placing the patient's arms overhead or by using the SBF and diaphragm press or Abches. However, this was not true for all the patients, because there were those whose range of tumor motion became worse in the setups other than the reference setup. Because of the small number of patients, we grouped the tumors into two categories: upper lobe and middle or lower lobe. In the reference setup, the CC direction yielded a significant difference in the mean effective range of the upper and middle or lower lobe markers, with a $p$ value of 0.02. On the other hand, the differences in the mean effective range of markers in the upper lobe and the middle or lower lobes were not statistically significant for either the LR or AP direction in the reference setup.

We compared the effectiveness of each setup in reducing respiratory-induced intrafractional organ motion. Table 2

Table 2. Comparison between the mean effective ranges of motion (±1 SD) of the markers in the upper and middle or lower lobes for the 5 patient setups evaluated

| | | LR | CC | AP |
|---|---|---|---|---|
| No SBF, arms down (nSBF_AD) | Upper | 2.15 ± 0.89 (0.60–3.20) | 4.59 ± 3.01 (0.93–9.53) | 3.39 ± 1.42 (1.00–5.87) |
| | Middle or lower | 2.18 ± 1.60 (0.60–5.27) | 10.93 ± 6.36 (1.07–19.93) | 4.33 ± 3.05 (1.13–10.20) |
| | *p* value | 0.66 | 0.02 | 0.72 |
| No SBF, arms up (nSBF_AU) | Upper | 2.21 ± 0.96 (0.67–3.73) | 4.51 ± 3.06 (0.87–10.13) | 3.23 ± 1.63 (1.00–6.27) |
| | Middle or lower | 2.55 ± 1.56 (0.67–5.60) | 10.6 ± 6.09 (1.07–19.00) | 3.91 ± 2.45 (1.33–8.27) |
| | *p* value | 0.72 | 0.03 | 0.72 |
| With SBF (wSBF) | Upper | 1.97 ± 0.89 (0.67–3.33) | 4.23 ± 2.76 (0.67–9.53) | 3.04 ± 1.54 (1.07–5.67) |
| | Middle or lower | 2.98 ± 2.41 (0.87–6.93) | 9.91 ± 5.67 (1.07–16.87) | 4.43 ± 3.63 (0.93–10.60) |
| | *p* value | 0.78 | 0.03 | 0.84 |
| With SBF + diaphragm press (wSBF + DP) | Upper | 1.95 ± 0.86 (0.60–3.33) | 3.77 ± 2.57 (0.80–8.60) | 3.09 ± 1.33 (1.20–5.27) |
| | Middle or lower | 2.53 ± 2.23 (0.73–7.60) | 9.43 ± 5.56 (0.80–16.33) | 3.61 ± 2.64 (0.67–8.93) |
| | *p* value | 0.90 | 0.03 | 0.97 |
| With SBF + Abches (wSBF + Ac) | Upper | 1.91 ± 0.81 (0.60–2.93) | 3.98 ± 2.68 (0.73–8.33) | 2.88 ± 1.23 (1.20–4.60) |
| | Middle or lower | 3.27 ± 2.70 (0.67–7.73) | 12.84 ± 6.37 (1.00–18.87) | 5.04 ± 4.81 (0.93–13.40) |
| | *p* value | 0.89 | 0.01 | 0.60 |

*Abbreviations:* LR = left-right; AP = anteroposterior; CC = craniocaudal; SBF = stereotactic body frame.
Given in brackets are the minimum and maximum effective ranges. The *p* values listed here are derived from the Mann-Whitney test.

shows the mean effective ranges of marker motion for all the patients in the five setups evaluated in this study. Also listed in Table 2 are the *p* values obtained from the nonparametric comparison of the mean effective marker range between the upper and the middle or lower groups of patients for each setup using the Mann-Whitney test. Measurements using these setups were carried out for all the patients except for 2 patients who decided not to continue with the measurements after the fourth setup. The sequences of setups for the tracking sessions were randomly changed between patients to minimize the possible bias from the setup sequence. Results of the RTRT measurement of the effective range of motion of fiducial markers showed that the use of the SBF, diaphragm press, or breathing cycle monitor to control the patient's breathing did not generally yield smaller effective marker ranges either for tumors in the upper lobe or those in the middle or lower lobes.

*Motion of markers in the upper lobe*

The mean effective ranges in the LR direction of the markers in the upper lobe showed little variation among the different patient setups. In the LR direction, they were around 2 mm for all setups (Fig. 3). The differences between the reference setup and the four other setups were no more than 1 mm, and none of these differences were statistically significant at the 5% level. Along the CC direction, the average effective ranges of the markers in the 5 setups were between 3.77 mm and 4.59 mm (Fig. 4). The mean and median of the effective range were around 2.88 mm to

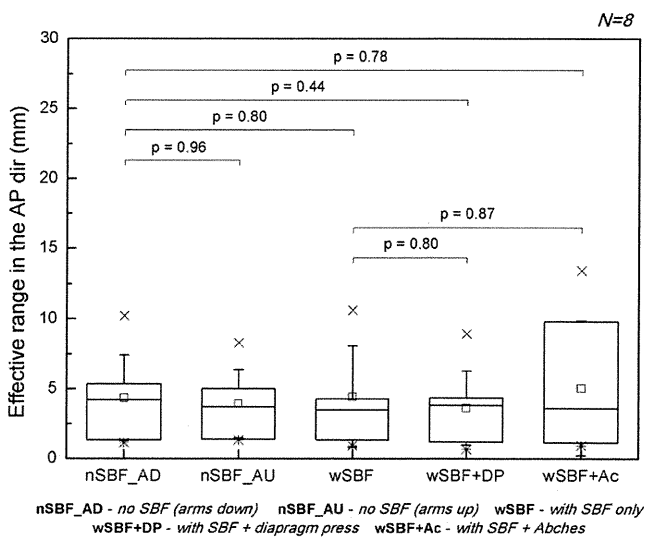


Fig. 3. The effective range along the lateral direction of the gold markers in the upper lobes of the lung. Also indicated are the *p* values obtained from comparison of the effective ranges obtained in each patient setup.

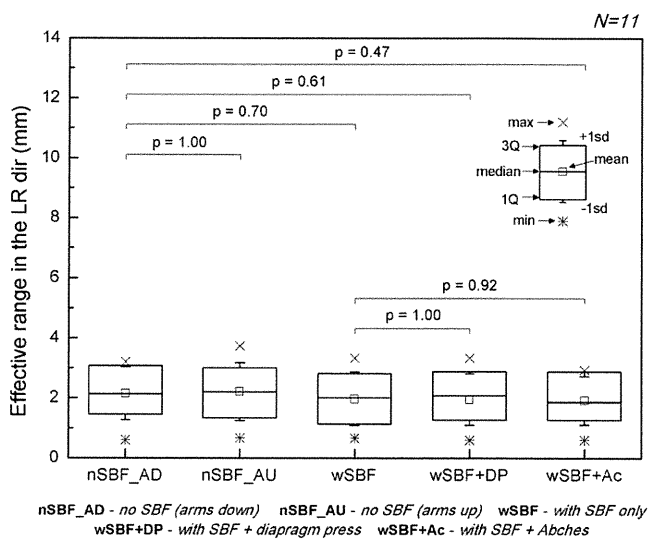


Fig. 4. The effective range along the craniocaudal direction of the gold markers in the upper lobes of the lung. Also indicated are the *p* values obtained from comparison of the effective ranges obtained in each patient setup.

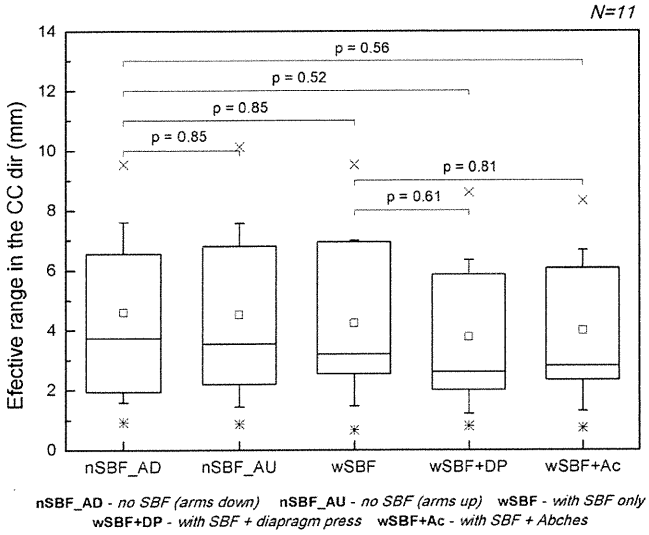


Fig. 5. The effective range along the anteroposterior direction of the gold markers in the upper lobes of the lung. Also indicated are the *p* values obtained from comparison of the effective ranges obtained in each patient setup.

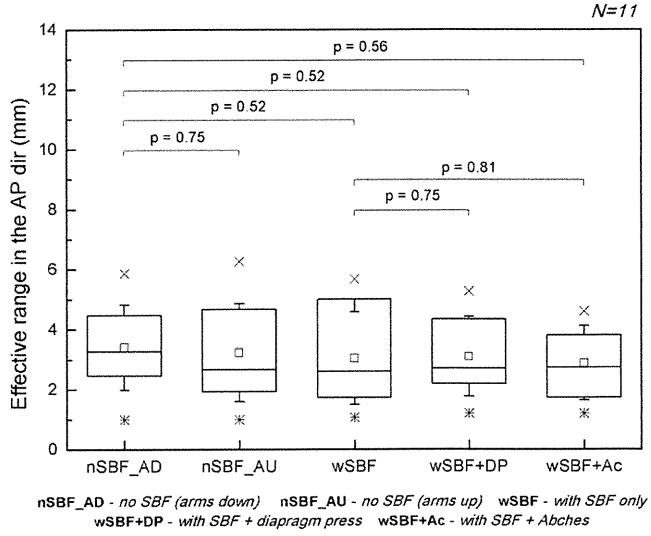


Fig. 6. The effective range along the lateral direction of the gold markers in the middle or lower lobes of the lung. Also indicated are the *p* values obtained from comparison of the effective ranges obtained in each patient setup.

3.39 mm in the AP direction (Fig. 5). The spread of the effective range values was largest along the CC direction, with a standard deviation of about 2.57–3.06 mm, and smallest along the LR direction, with a standard deviation of less than 1 mm. The maximum effective ranges of the markers obtained from the LR, CC, and AP directions were 3.73 mm, 10.13 mm, and 6.27 mm, respectively.

*Motion of markers in the middle or lower lobes*

As shown in Fig. 6, a slight variation in the mean effective range along the LR direction for the five setups was observed in the middle or lower lobe markers, with values between 2.18 mm and 2.98 mm; however, these differences were also not statistically significant (see The *p* values in Fig. 6).

The spread of the effective ranges for this group was greater than that for the upper lobe markers, which had standard deviations of 1.56–2.70 mm.

Shown in Fig. 7 are the effective ranges in the CC direction for the middle or lower lobe markers. Although the two setups without SBF had mean effective ranges greater than 10 mm and the mean effective ranges for the SBF setup and the SBF + diaphragm setup were less than 10 mm, the differences in the mean effective range between the setups were not statistically significant. The use of the Abches for this group of patients resulted in a mean effective range of about 13 mm. The standard deviations of the effective ranges in the CC direction were between 5.56 mm and 6.37 mm.

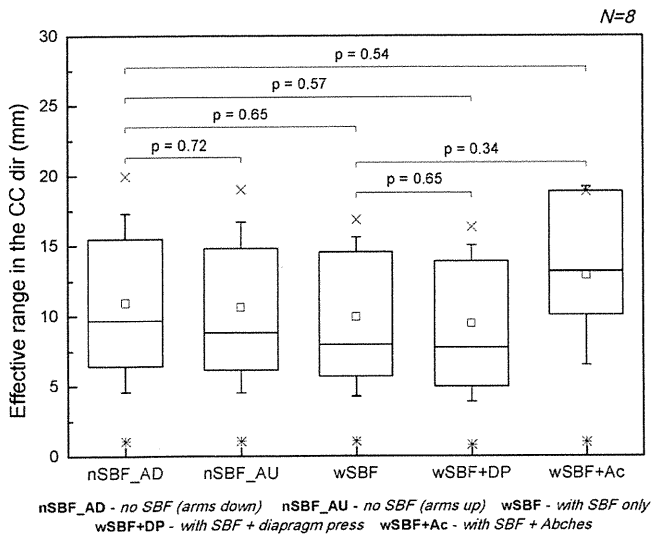


Fig. 7. The effective range along the craniocaudal direction of the gold markers in the middle or lower lobes of the lung. Also indicated are the *p* values obtained from comparison of the effective ranges obtained in each patient setup.

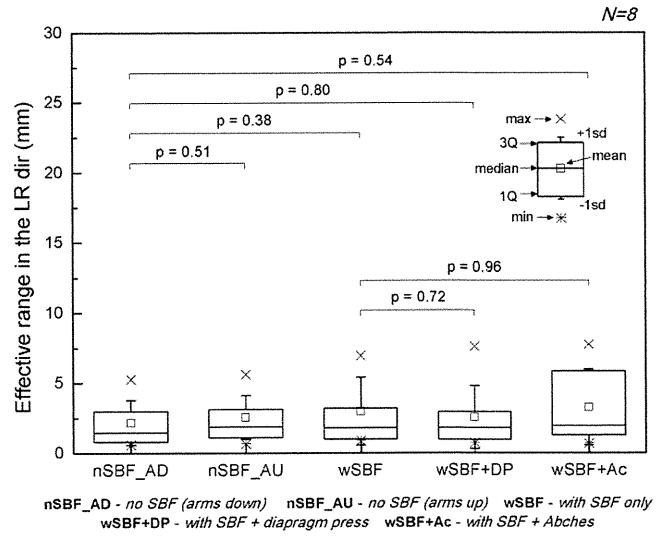


Fig. 8. The effective range along the anterior-posterior direction of the gold markers in the middle or lower lobes of the lung. Also indicated are the *p* values obtained from comparison of the effective ranges obtained in each patient setup.

The effective ranges in the AP direction for the middle or lower lobe markers were also greater than their upper lobe counterparts. The mean effective ranges shown in Fig. 8 for the five patient setups are between 3.61 mm and 5.04 mm with standard deviations between 2.45 mm and 4.81 mm. Again, no significant differences were noted among the five setups. The setup including the Abches had the largest mean effective range of 5.04 ± 4.81 mm.

## DISCUSSION

In the present study, the real-time tracking capability of our RTRT system was used to determine the three-dimensional motion of fiducial gold markers embedded near or at the tumor to determine whether the respiration-induced motion of these markers can be controlled in free and restricted breathing setups. With the RTRT system, we were able to determine the instantaneous displacement of fiducial markers near the tumor, as has been done in previous studies (7, 15, 19, 20), as well as the full range of motion of these markers. This allowed a more comprehensive evaluation of the feasibility of controlling respiratory-induced motion by using an SBF, diaphragm press and breathing cycle monitor.

The motions of fiducial markers were found to be highly patient-dependent and were influenced by the location where the markers were embedded in the lung. In general, markers in the upper lobes exhibited a smaller range of motions along the LR, CC, and AP directions compared with the motions of the markers in the lower lobes, which are consistent with the previous results reported by Seppenwoolde *et al.* (3) and Onimaru *et al.* (16). The average effective ranges of marker motion in the present study were comparable with the amplitudes obtained in the three-dimensional analysis by Seppenwoolde *et al.* (3) of tumor motion in the lung in a setup without SBF and with the patient's arms down.

The markers in the upper lobe of the lung exhibited ranges of motions, which did not vary significantly irrespective of the patient setup used. Additionally, their maximum effective ranges, which were all observed in the CC direction, were <10 mm. Engelsmann *et al.* (21) have previously reported that respiration-induced tumor motion of up to 10 mm does not drastically change the dose distribution. Thus, the patient breathing control may no longer be necessary for the majority of tumors in the upper lobes of the lung.

The markers in the middle or lower lobes of the lung exhibited larger motion in the CC direction and larger spread in the individual effective ranges in the LR, CC, and AP directions. Thus, respiration-induced tumor motion management for tumors in the lower lobes is worth considering, if possible (21).

We evaluated five patient setups in this study with the goal of reducing respiration-induced tumor motion; however, we found that the effective range of marker motions in the lower lobes of the lung was not significantly different among these setups. This result is different from the pioneering studies of Lax *et al.* (7) and Negoro *et al.* (9), which attempted to limit the abdominal motion of patients using the SBF and a diaphragm press. However, the comparisons between setups with or without a diaphragm press in the two aforementioned studies were done with a smaller number of patients compared with the present study (7, 8). Lax *et al.* noted that the diaphragmatic motion was reduced from a range of 1.5–2.5 cm to a range of 0.5–1.0 cm in 17 patients evaluated using fluoroscopy (7). Negoro *et al.* found that tumor motion in the CC direction was reduced from 8–20 mm for the setup with SBF down to only 2–10 mm for the setup using SBF and diaphragm press in 10 patients (9). However, they also had 1 patient whose tumor movement of 7 mm increased to 10 mm upon the use of diaphragm control. Compared with the previous visual measurement using AP fluoroscopy, the present study measured the three-dimensional motion of the internal fiducial markers with more objective and reproducible methods. Thus the discrepancy in the results between these pioneering works and the present study may have been related to the methods used or the precision of the measurements, together with other factors such as the patient background (*e.g.*, tumor stage, location of tumors).

Additionally, although the tracking sessions were performed using a random sequence of patient setups, this may not have completely eliminated some bias due to patient setup, since by the time the patient goes through the last setup, he or she would have been on the couch for at least 20 min longer compared with the first setup. We also cannot neglect the possibility that some patients might have benefited from any of the setups evaluated in this study because of the relatively small patient population. However, it is not possible from our study to recommend the use of the SBF alone or in combination with the diaphragm press or the Abches as a universally effective method to control respiratory intrafractional organ motion.

In conclusion, our RTRT measurement of the effective range of motion of fiducial markers showed that using the SBF, the diaphragm press, or a breathing cycle monitor for the purpose of controlling the patient breathing does not generally result in smaller effective marker ranges. Whether these patient setups will be effective in reducing respiratory-induced organ motion should be examined for individual patients before using them in the radiotherapy.

## REFERENCES

1. Keall PJ, Mageras GS, Balter JM, *et al.* The management of respiratory motion in radiation oncology report of AAPM Task Group 76. *Med Phys* 2006;33:3874–3900.
2. Shimizu S, Shirato H, Ogura S, *et al.* Detection of lung tumor movement in real-time tumor-tracking radiotherapy. *Int J Radiat Oncol Biol Phys* 2001;51:304–310.
3. Seppenwoolde Y, Shirato H, Kitamura K, *et al.* Precise and real-time measurement of 3D tumor motion in lung due to breathing

and heartbeat, measured during radiotherapy. *Int J Radiat Oncol Biol Phys* 2002;53:822–834.
4. Shirato H, Harada T, Harabayashi T, *et al.* Feasibility of insertion/implantation of 2.0 mm-diameter gold internal fiducial markers for precise setup and real-time tumor tracking in radiotherapy. *Int J Radiat Oncol Biol Phys* 2003;56: 240–247.
5. Shirato H, Shimizu S, Shimizu T, *et al.* Real-time tumour-tracking radiotherapy. *Lancet* 1999;353:1331–1332.
6. Shirato H, Shimizu S, Kunieda T, *et al.* Physical aspects of a real-time tumor-tracking system for gated radiotherapy. *Int J Radiat Oncol Biol Phys* 2000;48:1187–1195.
7. Lax I, Blomgren H, Naslund I, *et al.* Stereotactic radiotherapy of malignancies in the abdomen. *Acta Oncol* 1994;33:677–683.
8. Herfarth K, Debus J, Lohr F, *et al.* Extracranial stereotactic radiation therapy: Set-up accuracy of patients treated for liver metastases. *Int J Radiat Oncol Biol Phys* 2000;46: 329–335.
9. Negoro Y, Nagata Y, Aoki T, *et al.* The effectiveness of an immobilization device in conformal radiotherapy for lung tumor: Reduction of respiratory tumor movement and evaluation of the daily set-up accuracy. *Int J Radiat Oncol Biol Phys* 2001;50:889–898.
10. Ko Y, Suh Y, Ahn S, *et al.* Immobilization effect of air-injected blanket (AIB) for abdomen fixation. *Med Phys* 2005;32: 3363–1046.
11. Harada T, Shirato H, Ogura S, *et al.* Real-time tumor-tracking radiation therapy for lung carcinoma by the aid of insertion of a gold marker using bronchofiberscopy. *Cancer* 2002;95: 1720–1727.
12. Imura M, Yamazaki K, Shirato H, *et al.* Insertion of fiducial markers for setup and tracking of lung tumors in radiotherapy. *Int J Radiat Oncol Biol Phys* 2005;63:1442–1447.
13. Hof H, Herfarth K, Münter M, *et al.* Stereotactic single-dose radiotherapy of stage I non-small-cell lung cancer (NSCLC). *Int J Radiat Oncol Biol Phys* 2003;56:335–341.
14. Lohr F, Debus J, Frank C, *et al.* Non-invasive patient fixation for extracranial stereotactic radiotherapy. *Int J Radiat Oncol Biol Phys* 1999;45:521–527.
15. Nagata Y, Negoro Y, Aoki T, *et al.* Clinical outcomes of 3D conformal hypofractionated single high-dose radiotherapy for one of two lung tumors using a stereotactic body frame. *Int J Radiat Oncol Biol Phys* 2002;52:1041–1046.
16. Onimaru R, Shirato H, Fujino M, *et al.* The effect of tumor location and respiratory function on tumor movement estimated by real-time tracking radiotherapy (RTRT) system. *Int J Radiat Oncol Biol Phys* 2005;63:164–169.
17. Barnes E, Murray B, Robinson D, *et al.* Dosimetric evaluation of lung tumor immobilization using breath hold at deep inspiration. *Int J Radiat Oncol Biol Phys* 2001;50:1091–1098.
18. Shirato H, Oita M, Fujita K, *et al.* Feasibility of synchronization of real-time tumor-tracking radiotherapy and intensity-modulated radiotherapy from viewpoint of excessive dose from fluoroscopy. *Int J Radiat Oncol Biol Phys* 2004;60: 335–341.
19. Shirato H, Suzuki K, Sharp G, *et al.* Speed and amplitude of lung tumor motion precisely detected in four-dimensional setup and in real-time tumor-tracking radiotherapy. *Int J Radiat Oncol Biol Phys* 2006;64:1229–1236.
20. Mageras GS, Yorke E, Rosenzweig K, *et al.* Fluoroscopic evaluation of diaphragmatic motion reduction with a respiratory gated radiotherapy system. *J Appl Clin Med Phys* 2001;2: 191–200.
21. Engelsman M, Sharp G, Bortfeld T, Onimaru R, Shirato H. How much margin reduction is possible through gating or breath hold? *Phys Med Biol* 2005;50:477–490.

Int. J. Radiation Oncology Biol. Phys., Vol. ■, No. ■, pp. 1–7, 2010

0360-3016/$–see front matter

ELSEVIER

doi:10.1016/j.ijrobp.2009.07.1751

**CLINICAL INVESTIGATION**

# STEREOTACTIC BODY RADIOTHERAPY (SBRT) FOR OPERABLE STAGE I NON–SMALL-CELL LUNG CANCER: CAN SBRT BE COMPARABLE TO SURGERY?

Hiroshi Onishi, M.D.,* Hiroki Shirato, M.D.,† Yasushi Nagata, M.D.,‡ Masahiro Hiraoka, M.D.,§ Masaharu Fujino, M.D.,†* Kotaro Gomi, M.D.,‖ Katsuyuki Karasawa, M.D.,¶ Kazushige Hayakawa, M.D.,# Yuzuru Niibe, M.D.,# Yoshihiro Takai, M.D.,** Tomoki Kimura, M.D.,†† Atsuya Takeda, M.D.,‡‡ Atsushi Ouchi, M.D.,§§ Masato Hareyama, M.D.,‖‖ Masaki Kokubo, M.D.,¶¶ Takuyo Kozuka, M.D.,## Takuro Arimoto, M.D.,*** Ryusuke Hara, M.D.,††† Jun Itami, M.D.,‡‡‡ and Tsutomu Araki, M.D.*

*School of Medicine, Yamanashi University, Yamanashi, Japan; †School of Medicine, Hokkaido University, Sapporo, Japan; ‡School of Medicine, Hiroshima University, Hiroshima, Japan; §School of Medicine, Kyoto University, Kyoto, Japan; ‖Cancer Institute Suwa Red-Cross Hospital, Suwa, Japan; ¶Tokyo Metropolitan Komagome Hospital, Tokyo, Japan; #Kitasato University, Kanagawa, Japan; **School of Medicine, Hirosaki University, Hirosaki, Japan; ††School of Medicine, Kagawa University, Hiroshima, Japan; ‡‡Ofuna Chuo Hospital, Kanagawa, Japan; §§Keijinkai Hospital, Sapporo, Japan; ‖‖Sapporo Medical University, Sapporo, Japan; ¶¶Institute of Biomedical Research and Innovation, Kobe, Japan; ##School of Cancer Institute Ariake Hospital, Tokyo, Japan; ***Kitami Red Cross Hospital, Kitami, Japan; †††National Institute of Radiological Science, Chiba, Japan; and ‡‡‡National Cancer Center, Tokyo, Japan

**Purpose: To review treatment outcomes for stereotactic body radiotherapy (SBRT) in medically operable patients with Stage I non–small-cell lung cancer (NSCLC), using a Japanese multi-institutional database.**

**Patients and Methods: Between 1995 and 2004, a total of 87 patients with Stage I NSCLC (median age, 74 years; T1N0M0, $n = 65$; T2N0M0, $n = 22$) who were medically operable but refused surgery were treated using SBRT alone in 14 institutions. Stereotactic three-dimensional treatment was performed using noncoplanar dynamic arcs or multiple static ports. Total dose was 45–72.5 Gy at the isocenter, administered in 3–10 fractions. Median calculated biological effective dose was 116 Gy (range, 100–141 Gy). Data were collected and analyzed retrospectively.**

**Results: During follow-up (median, 55 months), cumulative local control rates for T1 and T2 tumors at 5 years after SBRT were 92% and 73%, respectively. Pulmonary complications above Grade 2 arose in 1 patient (1.1%). Five-year overall survival rates for Stage IA and IB subgroups were 72% and 62%, respectively. One patient who developed local recurrences safely underwent salvage surgery.**

**Conclusion: Stereotactic body radiotherapy is safe and promising as a radical treatment for operable Stage I NSCLC. The survival rate for SBRT is potentially comparable to that for surgery.** © **2010 Elsevier Inc.**

**Stereotactic body radiotherapy, Lung cancer, Non–small-cell, Operable, Stage I.**

## INTRODUCTION

With the popularization of computed tomography (CT) screening, lung cancers are increasingly detected at an early stage. For patients with Stage I (T1 or 2, N0, M0) non–small-cell lung cancer (NSCLC), resection of the set of full lobar and systemic lymph nodes represents standard treatment. Five-year overall survival rates for clinical Stage IA and IB treated surgically are approximately 60–75% and 40–60%, respectively (1–3). However, a proportion of patients who meet the criteria for surgery refuse such intervention for various reasons. Radiotherapy offers a therapeutic alternative in such cases, but the effects of conventional radiotherapy in patients with Stage I NSCLC are unsatisfactory, with local control rates of approximately 50% during a short 5-year survival period in 15–30% of patients (4–7). Survival rates for conventional radiotherapy for a statistically sufficient number of cases of operable Stage I NSCLC have not been reported, because most

Reprint requests: Hiroshi Onishi, M.D., Department of Radiology, School of Medicine, University of Yamanashi, 1110 Shimokato, Chuo City, Yamanashi 409-3898, Japan. Tel: (+81) 55-273-1111, ext 2382; Fax: (+81) 55-273-6744; E-mail: honishi@yamanashi.ac.jp

Presented at the 43rd Annual Meeting of the American Society of Clinical Oncology, June 1–7, 2007, Chicago, IL; and the 49th Annual Meeting of the American Society of Therapeutic Radiology and Oncology, October 28–November 1, 2007, Los Angeles, CA.

Supported in part by a Grant-in-Aid from the Ministry of Health, Welfare and Labor of Japan.

Conflict of interest: none.

*Acknowledgments*—The authors thank the patients and staff who assisted in this study.

Received May 7, 2009, and in revised form July 21, 2009. Accepted for publication July 22, 2009.

patients receiving radiotherapy are inoperable. The poor local control rates with conventional radiotherapy have been attributed to doses of conventional radiotherapy that are too low to control the tumor. Mehta *et al.* (8) provided a detailed theoretical analysis of NSCLC responses to radiotherapy and a rationale for dose escalation. They concluded that higher biologically effective doses (BED) irradiated during a short period must be administered to achieve successful local control of lung cancer. To provide a higher dose to the tumor without increasing adverse effects, three-dimensional conformal radiotherapy techniques have been used, and better local control and survival have recently been reported (9–11). Over the last decade, hypofractionated high-dose stereotactic body radiotherapy (SBRT) has been actively performed for early-stage lung cancer, particularly in Japan (12–17). We have previously reported preliminary results for a Japanese multi-institutional review of 257 patients with Stage I NSCLC treated with SBRT (18). The results showed that local control and survival rates were better with BED ≥100 Gy than with <100 Gy, and survival rates were much better for medically operable patients than for medically inoperable patients. These results were encouraging, but the duration of follow-up for the study was somewhat short (median, 38 months), and we have not presented a detailed analysis of medically operable patients as a distinct subgroup. Although the standard therapy for operable Stage I NSCLC remains surgery, the effect of SBRT on medically operable patients is an issue of great concern. We provide herein detailed and matured results of SBRT (BED ≥100 Gy) for medically operable patients with Stage I NSCLC, using a retrospectively collected Japanese multi-institutional database.

## PATIENTS AND METHODS

*Eligibility criteria*

All patients who satisfied the following eligibility criteria were retrospectively collected from 14 major Japanese institutions in which SBRT for lung cancer was actively performed: (*1*) identification of T1N0M0 or T2N0M0 primary lung cancer on chest and abdominal CT, bronchoscopy, bone scintigraphy, or brain magnetic resonance imaging; (*2*) histopathologic confirmation of NSCLC; (*3*) medically operable cancer but selection of SBRT after refusal to undergo surgery. Medical operability was discussed within the multidisciplinary tumor board of each institution according to respiratory function, age, and complicating diseases. Basic cutoff values for medical operability were World Health Organization performance status ≤2, pressure of arterial oxygen ≥65 mm Hg, predicted postoperative forced expiratory volume in 1 s ≥800 mL, no heart failure requiring pharmacotherapy, no diabetes requiring insulin, no severe arrhythmia, and no history of cardiac infarction. Positron emission tomography was not essential in the staging procedures.

Patients were informed of the concept, methodology, and rationale of this treatment, which was performed in accordance with the 1983 revision of the Declaration of Helsinki.

Table 1. Patient characteristics

| | |
|---|---|
| Number (14 institutions) | 87 |
| Male | 63 |
| Female | 24 |
| Age (y), median (range) | 74 (43–87) |
| ECOG performance status | |
| 0 | 51 |
| 1 | 30 |
| 2 | 6 |
| Histology | |
| Adenocarcinoma | 54 |
| Squamous cell carcinoma | 25 |
| Other | 8 |
| Stage | |
| IA | 64 |
| IB | 23 |
| Tumor diameter (mm), median (range) | 25 (7–50) |
| IA | 21 |
| IB | 39 |
| Chronic lung disease | |
| Positive | 38 |
| Negative | 49 |

*Abbreviation:* ECOG = Eastern Cooperative Oncology Group.
Values are number unless otherwise noted.

*Patient characteristics*

A summary of patient pretreatment characteristics is given in Table 1. From April 1995 to March 2004, a total of 87 medically operable patients with primary NSCLC were treated using hypofractionated high-dose SBRT in 14 major Japanese institutions. Each of these 87 cases was judged medically operable, and surgery was initially recommended, but the patients declined surgery and selected SBRT as a radical treatment. Pathology of all tumors was confirmed as NSCLC by transbronchial or CT-guided percutaneous biopsy. The 14 participating institutions were these: Hokkaido University; Kyoto University; Cancer Institute Hospital; Tokyo Metropolitan Komagome Hospital; Kitasato University; Tohoku University; Hiroshima University; Tokyo Metropolitan Hiroo Hospital; Sapporo Medical University; Institute of Biomedical Research and Innovation; International Medical Center of Japan; Tenri Hospital; Kitami Red Cross Hospital; and Yamanashi University.

*Treatment methods*

Although the techniques to accomplish stereotactic methods differed among these institutions, all "stereotactic radiotherapy techniques" fulfilled the following five requirements: (*1*) reproducibility of the isocenter (setup error ≤5 mm), as confirmed by image guidance for every fraction; (*2*) respiratory motion (internal margin) suppressed using as much as possible, to <5 mm; (*3*) slice thickness on CT ≤3 mm for three-dimensional treatment planning; (*4*) irradiation with multiple noncoplanar static ports or dynamic arcs; and (*5*) single high dose ≥5 Gy.

Gross target volume (GTV) was delineated on CT images displayed with a lung window level. Clinical target volume (CTV) marginally exceeded GTV by 0–5 mm as judged by the individual radiation oncologist. Internal margin was

calculated and set around the CTV by 2–5 mm according to the individual measurements for respiratory motion of each institution. Internal margin caused by respiratory motion was reduced by gating, tracking, breath-hold technique, or abdominal compression. Planning target volume (PTV) comprised the CTV, a proper internal margin measured in each patient, and a 5-mm safety margin. The total margin between PTV and GTV was thus 7–15 mm. The irradiated port marginally exceeded PTV by 3–5 mm to secure the surface dose of PTV. Dose calculation was performed using the Clarkson algorithm and heterogeneity correction. A total dose of 45–72.5 Gy (mean, 58.7 Gy) at the isocenter in 3–10 fractions with single doses of 6.25–15 Gy was administered with 6-MV X-rays within 20% heterogeneity in the PTV dose. Minimum dose in the PTV corresponded to 85–95% of the prescribed dose in most cases. Typical dose/fractionation schedules were 75 Gy in 10 fractions for 42 patients and 48 Gy in 4 fractions for 38 patients. In principal, patients were treated on consecutive days, but some patients were treated every other day. No chemotherapies were administered before or during radiotherapy.

To compare the effects of various treatment protocols with different fraction sizes and total doses, BED was utilized in a linear-quadratic model (19). Biologically effective dose was here defined as $nd(1 + d/\alpha/\beta)$, with units of Gy, where $n$ is fractionation number, $d$ is daily dose, and $\alpha/\beta$ is assumed to be 10 for tumors. Biologically effective dose was not corrected with values for tumor doubling time or treatment term. Biologically effective dose was calculated at the isocenter in this study. Median calculated BED was 116 Gy (range, 100–141 Gy).

No restriction was placed on whether the tumor was located peripherally or centrally in the lung, but dose for the spinal cord was limited. Biologically effective dose limitation for spinal cord was 80 Gy ($\alpha/\beta$ was assumed to be 2 Gy for chronic spinal cord toxicity). Doses for other organs were not restricted.

*Evaluation*

The objectives of this study were to retrospectively evaluate toxicity, local control rate, and survival rate. Follow-up examinations were performed 4 weeks after treatment first, then patients were seen every 1–3 months. Tumor response was evaluated using the Response Evaluation Criteria in Solid Tumors by CT (20). Chest CT (slice thickness, 2–5 mm) was usually obtained every 2 to 3 months for the first year and repeated every 4–6 months thereafter. Complete response indicated that the tumor had completely disappeared or was judged to have been replaced by fibrotic tissue. Partial response was defined as a ≥30% reduction in maximum cross-sectional diameter. Distinguishing between residual tumor tissue and radiation fibrosis was difficult. Any suspicious residual confusing density after radiotherapy was considered evidence of partial response, so actual complete response rate may have been higher than presented herein. Distinguishing between local recurrence and inflammatory change was also difficult. Here, local recurrence was considered to have occurred only when enlargement of the local tumor continued for >6 months on follow-up CT, obviously positive findings were identified on positron emission tomography, or histologic confirmation was acquired. Findings on CT were interpreted by two radiation oncologists in each case. Absence of local recurrence was defined as locally controlled disease. Lung, esophagus, bone marrow, and skin were evaluated using version 2 of the National Cancer Institute–Common Toxicity Criteria.

*Statistical analysis*

Cumulative rates of progression-free status at local, regional lymph node, and distant sites and survival were calculated and drawn using Kaplan-Meier algorithms, with day of treatment as the starting point. Subgroups were compared using log–rank statistics. Values of $p < 0.05$ were considered statistically significant. Statistical calculations were conducted using StatView version 5.0 software (SAS Institute, Cary, NC).

## RESULTS

All patients completed treatment without obvious complaints. Median durations of observation for all patients and survivors as of final follow-up were 55 and 63 months, respectively.

*Local tumor response*

Complete response was achieved in 28 patients (32.2%), and partial response was seen in 43 patients (49.4%).

*Toxicity*

Radiation-induced pulmonary complications of National Cancer Institute–Common Toxicity Criteria (version 2.0) Grade 0, 1, 2, and 3 were noted in 21 (24.1%), 61 (70.1%), 4 (4.6%), and 1 patient (1.1%), respectively. Rib fracture and Grade 3 dermatitis were observed in 4 (4.6%) and 3 patients (3.4%), respectively. All tumors bordered the chest wall. Grade 3 radiation-induced esophagitis was produced in 1 patient, in whom the tumor slightly bordered the esophagus. Maximum esophageal dose in this case was 30 Gy in 5 fractions. No vascular, cardiac, or bone marrow complications had been encountered as of last follow-up. In total, Grade 3 toxicities were identified in 8 patients (9.2%).

No definite second malignancies were found during follow-up, but 1 patient died of acute myelogenous leukemia 3.7 years after completing SBRT.

*Recurrence*

Local recurrence, lymph node metastases, and distant metastases occurred in 8 (9.2%), 13 (14.9%), and 19 cases (21.8%), respectively.

Cumulative local progression–free rate curves according to stage are shown in Fig. 1. Cumulative local progression–free rate after 5 years was 86.7% (95% confidence interval [CI], 78.3–94.9%) for total cases. Cumulative local progression–free rate at 5 years was 92.0% (95% CI, 83.8–99.6%)

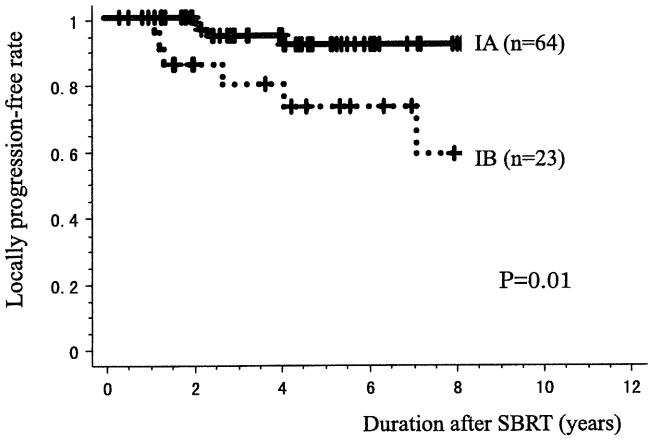


Fig. 1. Cumulative local progression–free rate curves, according to stage. SBRT = stereotactic body radiotherapy.

for the Stage IA subgroup, significantly superior ($p = 0.01$) to that for the Stage IB subgroup (73.0%; 95% CI, 52.2–93.7%). Five-year local progression–free rates were not significantly different between adenocarcinoma (80.9%; 95% CI, 68.7–93.1%) and squamous cell carcinoma (95.5%; 95% CI, 86.7–100.0%). One patient who developed local recurrence underwent surgery and has remained healthy for more than 3 years after operatively. The operation method was upper lobectomy and mediastinal lymphadenectomy, and they were performed safely without any trouble.

Cumulative curves of regional lymph node and distant metastases–free rates according to stage are shown in Figs. 2 and 3, respectively. The 5-year lymph node metastasis–free rate and distant metastasis–free rate for total cases was 85.3% (95% CI, 77.6–93.0%) and 75.1% (95% CI, 64.8–85.4%], respectively. No significant difference was identified between Stage IA and IB subgroups.

In patterns of regional nodal recurrence, 8 patients (61.5%) showed nodal failure alone, 2 patients (15.4%) had nodal failure combined with local failure, and 3 patients (23.1%) showed nodal failure combined with distant metastases.

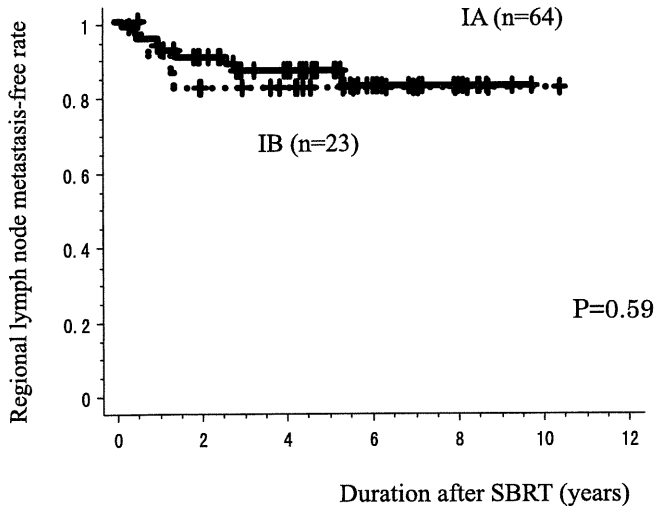


Fig. 2. Cumulative regional lymph node metastasis–free rate curves, according to stage. SBRT = stereotactic body radiotherapy.

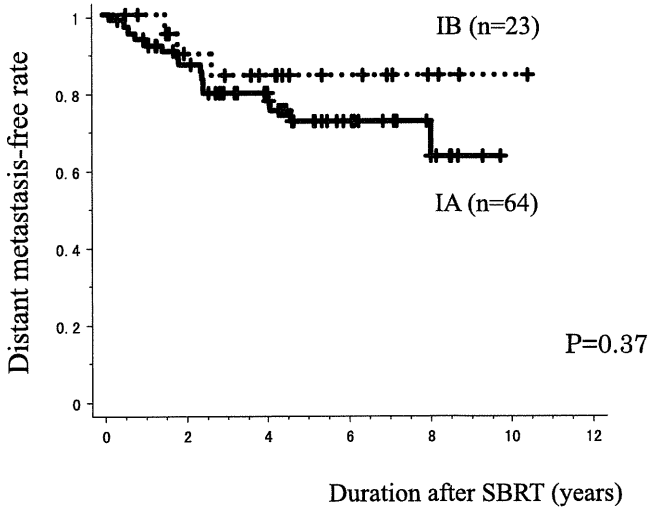


Fig. 3. Cumulative distant metastasis–free rate curves, according to stage. SBRT = stereotactic body radiotherapy.

*Survival*

Overall and cause-specific 5-year survival rates for total cases were 69.5% (95% CI, 58.8–80.1%) and 76.1% (95% CI, 65.9–86.3%), respectively. Overall and cause-specific survival curves according to stage are shown in Figs. 4 and 5, respectively. Five-year overall survival rate was 72.0% (95% CI, 59.6–84.4%) in Stage IA patients and 63.2% (95% CI, 42.7–83.6%) in Stage IB patients. A marginal but nonsignificant ($p = 0.14$) difference was found between overall survival rates of Stage IA and IB groups. In terms of histology, overall 5-year survival rate was 72.2% (95% CI, 59.2–85.2%) in the adenocarcinoma subgroup and 60.8% (95% CI, 38.4–83.2%) in the squamous cell carcinoma subgroup.

## DISCUSSION

Exposing a tumor to a higher dose of radiation without increasing adverse effects can be achieved using stereotactic techniques. Stereotactic irradiation is an approach using

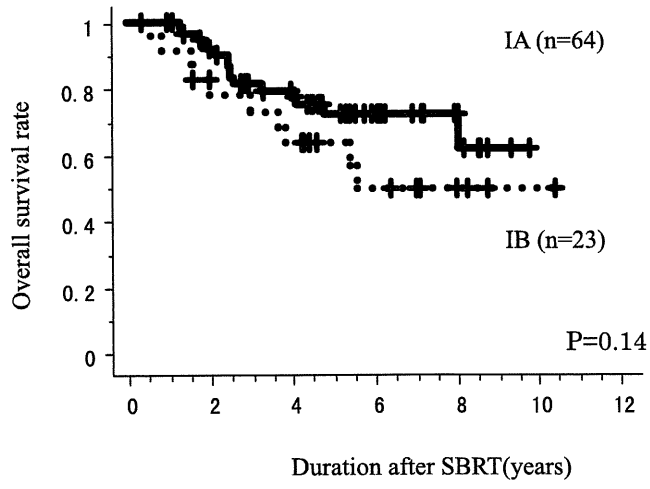


Fig. 4. Cumulative overall survival rate curves, according to stage. SBRT = stereotactic body radiotherapy.

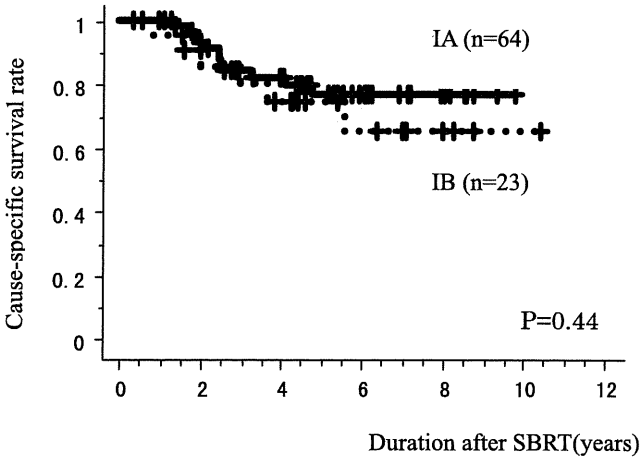


Fig. 5. Cumulative cause-specific survival rate curves, according to stage. SBRT = stereotactic body radiotherapy.

multiple noncoplanar convergent beams, precise localization with a stereotactic coordinate system, rigid immobilization, and single high-dose treatment, maximizing delivery to the tumor and minimizing the exposure of normal tissue. This approach can also substantially reduce overall treatment time from several weeks of conventional radiotherapy schedule to a few days, offering an important advantage to the patient. Stereotactic irradiation techniques are well established for the treatment of intracranial malignancies, but use in extracranial malignancies has been considered problematic because of the issues of fixation and internal motion. In 1994, Blomgren *et al.* (21) described a technique of SBRT using a custom-made body cast and stereotactic coordinates. In 1996, Uematsu *et al.* (22) reported a CT–linear accelerator unit sharing a common couch, enabling image-guided fractionated SBRT without rigid immobilization. Since verification of the effects and safety of SBRT for lung cancer (12), this treatment method has rapidly been adopted in many institutions (Table 2) (12–17, 23, 24). Although various fractionation schedules are undergoing evaluation around the world, a frequently used BED prescribed for tumors with SBRT for Stage I NSCLC in Japan has been set at a little over 100 Gy, as recommended in our previous study (18). However, concerning determination of the truly optimal dose of SBRT for Stage I NSCLC, many problems and controversies remain, such as dose-calculation algorithms (16), inhomogeneity corrections, essential dose for tumor control (24), and dose constraints for organs at risk (25, 26).

Although a number of articles on SBRT for Stage I NSCLC have been published, duration of follow-up in most cases has not been sufficiently long, and almost all treated patients were medically inoperable. The present study thus provides data on two important areas.

One was cumulative local recurrence and metastatic rates with a long duration of follow-up after SBRT. Rates of local control and metastases depend largely on the duration of follow-up and generally deteriorate as the duration of follow-up increases. Furthermore, recurrence rates have been reported in numerous articles, but most of them were crudely calculated rate. We have presented 5-year cumulative local control, regional lymph node recurrence–free and distant metastasis–free rates, calculated using Kaplan-Meier methods. The local progression–free rate in our results was unsatisfactory, particularly for the T2 tumor subgroup. The Japanese Clinical Oncology Group (JCOG) has thus started a multi-institutional dose-escalation study for Stage IB NSCLC patients (JCOG 0702).

Another meaningful result was the overall survival rate with a longer follow-up duration, allowing comparison between SBRT and surgery. Although the survival rate in this study was less than in our previous reports, we consider this information worth reporting, because median duration of follow-up was almost 5 years. Uematsu *et al.* (12) reported a 3-year overall survival rate of 86% in 29 medically operable patients with Stage I NSCLC, but the number of patients was small, and follow-up duration was relatively short. Because the number of medically operable patients treated with SBRT was very small in individual institutions, the present study collated the data of operable patients from multiple institutions. Whether the survival rate of SBRT was lower than that of surgery could not be clarified from our results. Representative 5-year overall survival rates of surgery for clinical

Table 2. Reports of SBRT for Stage I NSCLC

| First author (reference) | *N* | Total dose (Gy) | Single dose (Gy) | BED (Gy) | Median follow-up (mo) | Local recurrence (%) | 3-y overall survival (%) |
|---|---|---|---|---|---|---|---|
| Uematsu (12) | 50 | 72 | 7.2 | 124 | 60 | 6* | 6 |
| Nagata (13) | 42 | 48 | 12 | 106 | 52 | 3* | 82 |
| Onimaru (14) | 28 | 48 | 12 | 106 | 27 | 36† | 82 (Stage IA)<br>32 (Stage IB) |
| Onishi (15) | 26 | 72 | 7.2 | 124 | 24 | 8* | 75 |
| Takeda (16) | 63 | 50 | 10 | 100 | 31 | 5† | 90 (Stage IA)<br>63 (Stage IB) |
| Koto (17) | 31 | 45–60 | 7.5–15 | 105–113 | 32 | 29* | 72 |
| Hof (23) | 10 | 19–26 | 19–26 | 55–94 | 15 | 40* | 37 |
| Fakiris (24) | 47 | 60–66 | 20–22 | 180–211 | 50 | 12† | 43 |

*Abbreviations:* SBRT = stereotactic body radiotherapy; NSCLC = non–small-cell lung cancer; BED = biologically effective dose ($\alpha/\beta = 10$).
* Crude data.
† Cumulative data calculated with Kaplan-Meier method.

Table 3. Comparison of 5-y overall survival rate between surgical series and SBRT

| Clinical stage | United States (1) | Japanese National Cancer Center (2) | Japanese National Survey (3) | SBRT |
|---|---|---|---|---|
| IA | 61 | 71 | 77 | 76 |
| IB | 40 | 44 | 60 | 64 |

*Abbreviation:* SBRT = stereotactic body radiotherapy.
Values are percentages.

Stage IA and IB NSCLC are listed in Table 3 (1–3), ranging approximately 60–75% for Stage IA and 40–60% for Stage IB. We cannot conclude that the survival rate for SBRT is equivalent to that for surgery, because the present data for SBRT are based on a retrospective study and small sample size. However, the background of patients treated by SBRT in this study seems likely to have included worse prognostic factors than those in patients treated surgically. Concerning the size and characteristics of tumors, good prognostic factors such as smaller tumor size (27) or lower-density mass (so-called ground-glass opacities) (28) might be more frequently included in patients treated with surgery, because the determination of histological malignancy before SBRT was difficult for such tumors. In addition, median age of patients treated by surgery was approximately 10 years younger in the surgical series (median, 60–65 years) than in the SBRT series (median, 75 years). We therefore believe that survival rates for SBRT in medically operable patients are potentially comparable to those for surgery.

Regarding treatment-related toxicity, the rate of severe (Grade ≥3) acute and short-term chronic complications after SBRT was very low and acceptable, despite the high age of those patients (median, 74 years) in our experience. In results for pulmonary lobectomy, Deslauriers *et al.* (29) reported much higher mortality and morbidity rates that increased with aging. In other reports, mortality rates for patients aged >70 years old after pulmonary lobectomy were 7.6% (30). Even though improvements of mortality and morbidity of surgery may have recently been achieved (31), in particular under a technique of video-assisted thoracoscopic lobectomy (32), we consider SBRT as a safer and less invasive treatment modality than surgery, at least for peripherally located lung tumor up to 5 years after treatment. However, reports of SBRT for centrally located lung tumor have shown a comparably high risk (25, 26), and long-term chronic toxicity remains unclear. A longer and larger follow-up of SBRT is needed.

We thus consider that SBRT may offer a useful option for initial radical treatment of at least peripheral Stage IA NSCLC, not only for medically inoperable patients but also for operable patients. However, regarding centrally located or large T2 tumors, surgery must still be recommended as the first choice of treatment until further data can be accumulated. Although we encountered only 1 case in the present study, pulmonary lobectomy and mediastinal lymph node resection were performed without difficulty for a locally recurring tumor after SBRT. Surgery might be an option as salvage therapy for locally recurrent cases after radical SBRT for Stage I NSCLC.

In Japan, the number of patients treated with SBRT has exploded, especially since SBRT for lung cancer has been covered by the national health insurance since 2004. A Phase II multi-institutional study of JCOG researching the efficacy and toxicity of SBRT for both medically operable and inoperable Stage IA NSCLC patients (JCOG 0403) started in 2004, and patient entry was completed in October 2008. A total of 90 medically inoperable and 65 operable patients have been enrolled. In the United States, a Phase II multi-institutional study of SBRT for only medically inoperable Stage I NSCLC patients (Radiation Therapy Oncology Group 0236) has been ongoing.

Even multi-institutional Phase II studies of SBRT for Stage I NSCLC may have inevitable selection bias compared with surgical series. A prospective randomized trial is essential to conclude whether outcomes of SBRT for medically operable patients are truly comparable to those of surgery. A protocol for randomized studies comparing SBRT with surgery for Stage I NSCLC has been initiated (33) but has not progressed. Such a randomized study is likely to prove very difficult to perform, because most patients may hope for more minimally invasive therapy, such as SBRT. Many more experiences for more patients with a longer follow-up duration are thus needed to confirm the safety and effects of SBRT as a radical treatment for operable Stage I NSCLC. If the experience of SBRT for medically operable Stage I NSCLC matures and produces no poor results in future, SBRT will have a marked impact on standard treatment procedures for lung cancer and provide good news for Stage I lung cancer patients, the prevalence of whom is likely to increase.

In conclusion, treatment results of SBRT reviewed from a Japanese multi-institutional database showed that SBRT is safe and promising as a radical treatment for operable Stage I NSCLC. The survival rate of SBRT is potentially comparable to that of surgery.

## REFERENCES

1. Mountain CF. The international system for staging lung cancer. *Semin Surg Oncol* 2000;18:106–115.
2. Naruke T, Tsuchiua R, Kondo H, *et al.* Prognosis and survival after resection for bronchogenic carcinoma based on the 1997 TNM-staging classification: The Japanese experience. *Ann Thorac Surg* 2001;71:1759–1764.
3. Asamura H, Goya T, Koshiishi Y, *et al.* A Japanese Lung Cancer Registry study: Prognosis of 13,010 resected lung cancers. *J Thorac Oncol* 2007;3:46–52.
4. Sibley GS, Jamieson TA, Marks LB, *et al.* Radiotherapy alone for medically inoperable stage I non-small-cell lung cancer: The Duke experience. *Int J Radiat Oncol Biol Phys* 1998;40:149–154.

5. Krol AD, Aussems P, Noordijk EM, *et al.* Local irradiation alone for peripheral stage I lung cancer: Could we omit the elective regional nodal irradiation? *Int J Radiat Oncol Biol Phys* 1996;34:297–302.
6. Hayakawa K, Mitsuhashi N, Saito Y, *et al.* Limited field irradiation for medically inoperable patients with peripheral stage I non-small cell lung cancer. *Lung Cancer* 1999;26:137–142.
7. Jeremic B, Shibamoto Y, Acimovic L, *et al.* Hyperfractionated radiotherapy alone for clinical stage I nonsmall cell lung cancer. *Int J Radiat Oncol Biol Phys* 1998;38:521–525.
8. Mehta M, Scringer R, Mackie R, *et al.* A new approach to dose escalation in non-small cell lung cancer. *Int J Radiat Oncol Biol Phys* 2001;49:23–33.
9. Kong FM, Haken RK, Schipper MJ, *et al.* High-dose radiation improved local tumor control and overall survival in patients with inoperable/unresectable non-small cell lung cancer: Long-term results of a radiation dose escalation study. *Int J Radiat Oncol Biol Phys* 2005;63:324–333.
10. Narayan S, Henning GT, Haken RK, *et al.* Results following treatment to dose of 92.4 or 102.9 Gy on a phase I dose escalation study for non-small cell lung cancer. *Lung Cancer* 2004;44: 79–88.
11. Fang LC, Komaki R, Allen P. Comparison of outcomes for patients with medically inoperable Stage I non-small-cell lung cancer treated with two-dimensional vs. three-dimensional radiotherapy. *Int J Radiat Oncol Biol Phys* 2006;66:108–116.
12. Uematsu M, Shioda A, Suda A, *et al.* Computed tomography-guided frameless stereotactic radiography for stage I non-small-cell lung cancer: 5-year experience. *Int J Radiat Oncol Biol Phys* 2001;51:666–670.
13. Nagata Y, Takayama K, Matsuo Y, *et al.* Clinical outcomes of a phase I/II study of 48Gy of stereotactic body radiotherapy in 4 fractions for primary lung cancer using a stereotactic body frame. *Int J Radiat Oncol Biol Phys* 2005;63:1427–1431.
14. Onimaru R, Fujino M, Yamazaki K, *et al.* Steep dose-response relationship for stage I non-small-cell lung cancer using hypofractionated high-dose irradiation by real-time tumor-tracking radiotherapy. *Int J Radiat Oncol Biol Phys* 2008;70:374–381.
15. Onishi H, Kuriyama K, Komiyama T, *et al.* Clinical outcomes of stereotactic radiotherapy for stage I non-small cell lung cancer using a novel irradiation technique: Patient self-controlled breath-hold and beam switching using a combination of linear accelerator and CT scanner. *Lung Cancer* 2004;45:45–55.
16. Takeda A, Sanuki N, Kunieda E, *et al.* Stereotactic body radiotherapy for primary lung cancer at a dose of 50Gy total in five fractions to the periphery of the planning target volume calculated using a superposition algorithm. *Int J Radiat Oncol Biol Phys* 2009;73:442–448.
17. Koto M, Takai Y, Ogawa Y, *et al.* A phase II study on stereotactic body radiotherapy for stage I non-small cell lung cancer. *Radiother Oncol* 2007;85:429–434.
18. Onishi H, Shirato H, Nagata Y, *et al.* Hypofractionated stereotactic radiotherapy (HypoFXSRT) for stage I non-small cell lung cancer: Updated results of 257 patients in a Japanese multi-institutional study. *J Thorac Oncol* 2007;2(7 Suppl. 3): S94–S100.
19. Yaes RJ, Patel P, Maruyama Y. On using the linear-quadratic model in daily clinical practice. *Int J Radiat Oncol Biol Phys* 1991;20:1353–1362.
20. Therasse P, Arbuck SG, Eisenhauer EA, *et al.* New guidelines to evaluate the response to treatment in solid tumors. *J Natl Cancer Inst* 2000;92:205–216.
21. Blomgren H, Lax I, Naslund I, Svanstrom R. Stereotactic high dose fraction radiation therapy of extracranial tumors using an accelerator. Clinical experience of the first thirty-one patients. *Acta Oncol* 1995;34:861–870.
22. Uematsu M, Fukui T, Shioda A, *et al.* A dual computed tomography and linear accelerator unit for stereotactic radiation therapy: A new approach without cranially fixated stereotactic frame. *Int J Radiat Oncol Biol Phys* 1996;35:587–592.
23. Hof H, Herfarth KK, Munter M, *et al.* Stereotactic single-dose radiotherapy of stage I non-small-cell lung cancer (NSCLC). *Int J Radiat Oncol Biol Phys* 2003;56:335–341.
24. Fakiris AJ, McGarry RC, Yiannoutsos CT, *et al.* Stereotactic body radiation therapy forearly-stage non-small-cell lung carcinoma: four-year results of a prospective phase II study. *Int J Radiat Oncol Biol Phys* 2009;75:677–682.
25. Timmerman R, McGarry R, Yiannoutsos C, *et al.* Excessive toxicity when treating central tumors in phase II study of stereotactic body radiation therapy for medically inoperable early-stage lung cancer. *J Clin Oncol* 2006;24:4833–4849.
26. Song SY, Choi W, Shin SS, *et al.* Fractionated stereotactic body radiation therapy for medically inoperable stage I lung cancer adjacent to central large bronchus. *Lung Cancer* 2009;66:89–93.
27. Akakura N, Mori S, Okuda K, *et al.* Subcategorization of lung cancer based on tumor size and degree of visceral pleural invasion. *Ann Thorac Surg* 2008;86:1084–1091.
28. Asamura H, Suzuki K, Watanabe S, *et al.* A clinicopathological study of resected subcentimeter lung cancers: A favorable prognosis for ground glass opacity lesions. *Ann Thorac Surg* 2003; 76:1016–1022.
29. Deslauriers J, Ginsberg RJ, Dubois P, *et al.* Current operative morbidity associated with elective surgical resection for lung cancer. *Can J Surg* 1989;32:335–339.
30. Thomas P, Piraux M, Jacques LF, *et al.* Clinical patterns and trends of outcome of elderly patients with bronchogenic carcinoma. *Eur J Cardiothorac Surg* 1998;13:266–274.
31. Nagai K, Yoshida J, Nishimura M. Postoperative mortality in lung cancer patients. *Ann Thorac Cardiovasc Surg* 2007;13: 373–377.
32. Whitson BA, Groth SS, Duval SJ, *et al.* Surgery for early stage non-small cell lung cancer: A systematic review of the video-assisted thoracoscopic surgery versus thoracotomy approaches to lobectomy. *Ann Thorac Surg* 2008;86:2008–2016.
33. Hurkmans CW, Cuijpers JP, Largerwaard FJ, *et al.* Recommendations for implementing stereotactic radiotherapy in peripheral stage IA non-small cell lung cancer: Report from the Quality Assurance Working Party of the randomized phase III ROSEL study. *Radiat Oncol* 2009;4:1.

IOP PUBLISHING PHYSICS IN MEDICINE AND BIOLOGY

Phys. Med. Biol. **55** (2010) 4321–4333 doi:10.1088/0031-9155/55/15/009

# Image-guided adaptive gating of lung cancer radiotherapy: a computer simulation study

**Michalis Aristophanous[1], Joerg Rottmann[1], Sang-June Park[1], Seiko Nishioka[2], Hiroki Shirato[3] and Ross I Berbeco[1]**

[1] Department of Radiation Oncology, Brigham and Women's Hospital, Dana Farber Cancer Institute and Harvard Medical School, Boston, MA, USA
[2] Department of Radiology, NTT Hospital, Sapporo, Japan
[3] Department of Radiation Medicine, Hokkaido University School of Medicine, Sapporo, Japan

E-mail: maristophanous@lroc.harvard.edu

Received 22 October 2009, in final form 4 June 2010
Published 20 July 2010
Online at stacks.iop.org/PMB/55/4321

**Abstract**

The purpose of this study is to investigate the effect that image-guided adaptation of the gating window during treatment could have on the residual tumor motion, by simulating different gated radiotherapy techniques. There are three separate components of this simulation: (1) the 'Hokkaido Data', which are previously measured 3D data of lung tumor motion tracks and the corresponding 1D respiratory signals obtained during the entire ungated radiotherapy treatments of eight patients, (2) the respiratory gating protocol at our institution and the imaging performed under that protocol and (3) the actual simulation in which the Hokkaido Data are used to select tumor position information that could have been collected based on the imaging performed under our gating protocol. We simulated treatments with a fixed gating window and a gating window that is updated during treatment. The patient data were divided into different fractions, each with continuous acquisitions longer than 2 min. In accordance to the imaging performed under our gating protocol, we assume that we have tumor position information for the first 15 s of treatment, obtained from kV fluoroscopy, and for the rest of the fractions the tumor position is only available during the beam-on time from MV imaging. The gating window was set according to the information obtained from the first 15 s such that the residual motion was less than 3 mm. For the fixed gating window technique the gate remained the same for the entire treatment, while for the adaptive technique the range of the tumor motion during beam-on time was measured and used to adapt the gating window to keep the residual motion below 3 mm. The algorithm used to adapt the gating window is described. The residual tumor motion inside the gating window was reduced on average by 24% for the patients with regular breathing patterns and the difference was statistically significant ($p$-value = 0.01). The magnitude of the residual tumor motion depended on the regularity of the breathing pattern suggesting that

  

image-guided adaptive gating should be combined with breath coaching. The adaptive gating window technique was able to track the exhale position of the breathing cycle quite successfully. Out of a total of 53 fractions the duty cycle was greater than 20% for 42 fractions for the fixed gating window technique and for 39 fractions for the adaptive gating window technique. The results of this study suggest that real-time updating of the gating window can result in reliably low residual tumor motion and therefore can facilitate safe margin reduction.

(Some figures in this article are in colour only in the electronic version)

## 1. Introduction

Lung cancer has been the leading cause of cancer-related deaths in the past two decades (Jemal *et al* 2009). At the same time, it has seen one of the smallest improvements in survival in the past 30 years (13% to 16% improvement in 5 year survival). The primary treatment option for patients with non-small cell lung cancer is surgery, while the standard of care for inoperable lung cancer has been chemoradiotherapy. The survival of patients receiving concurrent chemoradiotherapy is quite low with one RTOG report estimating the 4 year survival at 21% (Curran *et al* 2003). While many of the patients fail distantly, over 80% of patients can also have a local failure after complete response (Arriagada *et al* 1991). This is suggestive of failure of radiation therapy to control the disease, since it is a form of localized therapy. Tumor motion due to respiration necessitates large margins to ensure tumor coverage, which in turn can set insufficient upper limits to the amount of dose that can be delivered, due to normal tissue toxicity. Furthermore, despite the large margins often used, the possibility of marginal misses is not insignificant due to the unpredictable nature of respiration and positioning errors. Successful management of tumor motion can not only reduce the possibility of a marginal miss, but can lead to sufficient margin reductions that can make dose escalation possible.

Different methods exist or are under development for the management of respiratory-induced tumor motion. The most widespread are utilization of an abdominal compression plate, respiratory gating and dynamic tumor tracking and delivery with the use of implanted fiducials. The abdominal compression plate is used to apply pressure on the diaphragm and force the patient to breathe though their chest, therefore limiting the effect of the diaphragm on the tumor motion (Murray *et al* 2007, Kontrisova *et al* 2006). This method is quite uncomfortable and cannot always be tolerated by patients, while at the same time it is not always effective in constraining the tumor motion. Dynamic MLC (DMLC) delivery uses implanted fiducials to track the tumor and deliver the dose at the location where the tumor is at any given point (Papiez *et al* 2005, Cho *et al* 2009, D'Souza *et al* 2005), by either adjusting the MLCs or moving the table. Problems with these approaches include accounting for system latency as well as the potential for errors associated with complex motions. Another motion management technique that has been developed in the last few years is to use external surrogates to obtain a respiratory signal and turn the beam on (gate) during a specific phase of the respiratory cycle (typically exhale). This technique is known as respiratory-gated radiotherapy. The advantage of such a method is that it is non-invasive and the only requirement for the patient is to breathe normally. The main disadvantage of gating is that it relies on an external signal to infer information about the internal location of the tumor, which may not always be accurate (Ionascu *et al* 2007, Berbeco *et al* 2005).

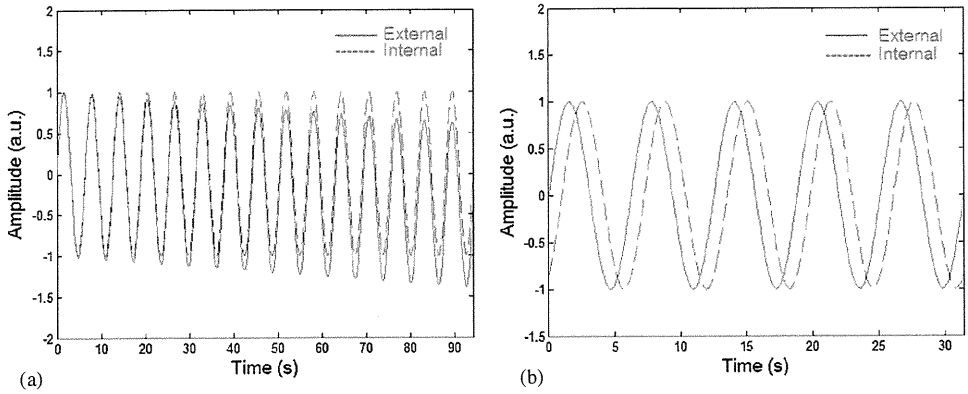


**Figure 1.** Two plots using sine waves to illustrate the main problems in respiratory gated radiotherapy: (a) a baseline drift where the external respiratory signal drifts downward and (b) a time shift between the external and internal signals.

The external respiratory signal can be obtained in a number of different ways; however, no matter which method is used the breathing signal can be quite irregular. This can make it difficult to accurately and consistently capture the exhale position during the entire treatment. Figure 1(a) illustrates the effect of a *baseline drift* (Nishioka *et al* 2008, Nottrup *et al* 2007, Hugo *et al* 2006, Sonke *et al* 2005). As the patient relaxes, the external signal can drift downward. At that point the gating has to be stopped and the gating window needs to be readjusted. This adds time and uncertainty to a gated treatment. If the gating window is not readjusted, the residual motion of the tumor can be greater than expected resulting in a marginal miss. It is also possible that the external signal may not be well correlated with the internal position of the tumor, as shown in figure 1(b), making it unreliable for guiding the treatment. This *time shift* has been previously demonstrated (Ionascu *et al* 2007, Chi *et al* 2006, Ford *et al* 2003, Vedam *et al* 2001) and it can also result in increased residual tumor motion. Effective ways of dealing with a time shift would be to add a time delay between the external and internal signals or to reduce the gating window. For either one of these remedies to work, the correlation between the internal and external signals needs to be well characterized and updated regularly, since the time shifts can vary from fraction to fraction (Ionascu *et al* 2007). Studies have shown that because of the issues mentioned above, gating cannot be safely used to reduce treatment margins (Nottrup *et al* 2007, Korreman *et al* 2008). In one study by Korreman *et al*, it was found that even with gating the reduction in the mean tumor motion was quite low (6%). They conclude that the only way to reduce the margins is by some form of image guidance.

With the advent of image-guided radiation therapy (IGRT) several methods have been proposed for improving patient setup and tracking the tumor (Wiersma *et al* 2008, Mao *et al* 2008, Adamson *et al* 2008, Purdie *et al* 2007). Both kV and MV imagers are routinely added to medical linear accelerators, making it possible to use extensive imaging both before treatment as part of setup and during treatment for verification. Some examples include fluoroscopy, radiographs and cone beam CT, all of which can be performed with kV or MV. MV fluoroscopy or *cine* EPID imaging can be performed during treatment to monitor tumor motion (Berbeco *et al* 2005, 2007). Markerless tumor tracking, both in MV and kV imaging, is a research area that has received increased attention in recent years (Rottmann *et al* 2009a, 2009b, Berbeco *et al* 2009, Xu *et al* 2008, Arimura *et al* 2009, Meyer *et al* 2006, Lin *et al* 2009).